

Long-term kinematics and sediment flux of an active earthflow, Eel River, California

B.H. Mackey^{1*}, J.J. Roering¹, and J.A. McKean²

¹Department of Geological Sciences, University of Oregon, Eugene, Oregon 97403, USA

²U.S. Department of Agriculture, Forest Service, Rocky Mountain Research Station, 322 E. Front Street, Suite 401, Boise, Idaho 83702, USA

ABSTRACT

Although earthflows are the dominant erosion mechanism in many mountainous landscapes, estimates of long-term earthflow-driven sediment flux remain elusive because landslide displacement data are typically limited to contemporary time periods. Combining high-resolution topography from airborne LiDAR (light detection and ranging), total station surveying, orthorectified historical aerial photographs, and inventories of meteoric ¹⁰Be in soil pits, we quantified ~150 years of slope movement on a 1.5-km-long earthflow in the Eel River catchment, northern California, United States. Using LiDAR-derived topography, we mapped the upper half of the earthflow into three distinct kinematic zones: an upslope source area, a long narrow transport zone, and a mid-slope compressional zone. From our air photo analysis (1944–2006), average velocities are fastest in the transport zone (1.7 m/a), slowest in the source zone (<1 m/a), and decrease monotonically over the past 30 years in all three zones. Meteoric ¹⁰Be inventories systematically increase with distance downslope of the source area, consistent with the notion that the elongate transport zone acts like a relatively undeformed soil conveyor that can be used to quantify long-term displacement. Because our ¹⁰Be-derived transport zone velocity of 2.1 m/a averages over the past 150 years, pre-1944 velocities likely approached 2.5 m/a, suggesting that twentieth century land-use practices have not increased rates of sliding. Although our results reveal a progressive decline in velocity that may reflect exhaustion of readily mobilized source material, velocities temporarily increased in the mid-twentieth century due to major hydrologic events. Given an average velocity of 2 m/a, the Kekawaka earthflow is deflating its source area over 20 times faster than the regional erosion rate, emphasizing the localized and vigorous role of active earthflows in landscape evolution.

INTRODUCTION

Large, slow-moving (<2 m/a), glacier-like earthflows are pervasive in many rapidly eroding landscapes worldwide, most commonly in fine-grained marine sediments. They are extremely problematic for land management and transport corridors, and represent major point sources of sediment to the channel network, yet we have little knowledge of earthflow behavior beyond the decadal scale. While factors such as precipitation, temperature, topographic loading, or toe erosion are widely recognized to influence motion (e.g., Keefer and Johnson, 1983), the geomorphic role of this style of slow, persistent mass wasting as an erosional process remains poorly constrained, especially when compared to other processes such as bedrock channel incision, debris flows, or soil creep (Dietrich and Perron, 2006). The majority of earthflow research has been directed at interpreting earthflow mechanics by determining movement patterns over seasonal to annual monitoring periods, and this approach yields excellent data on contemporary earthflow behavior (e.g., Coe et al., 2003; Iverson and Major, 1987; Zhang et al., 1991).

With notable exceptions (Bovis and Jones, 1992; Kelsey, 1978), comparatively little focus

has been applied to the longer-term evolution of individual earthflows. Active earthflows can deflate their source basins orders of magnitude faster than regional erosion rates (Kelsey, 1978); consequently, earthflow movement at a given location will likely be episodic. As such, active earthflows may compose a small percentage of the landscape, yet account for a large fraction of the regional sediment flux. Attesting to the ephemeral nature of earthflow activity, much of an earthflow-prone landscape is imprinted with ubiquitous subtle headscarps, toes, and deflated transport zones from multiple generations of earthflows and landslides in various stages of dormancy (e.g., Bovis and Jones, 1992). Factors controlling long-term earthflow evolution include availability of easily mobilized source material, base-level control, slope buttressing, climatic variability, and land-use practices. To better understand the relative importance of such factors on earthflow transport history and evolution, we aim to define the long-term sediment flux, kinematics, and topographic development of an individual earthflow.

EEL RIVER, NORTHERN CALIFORNIA

The coastal ranges of northern California are composed of penetratively sheared metasedimentary interbedded sandstone and argillite

of the Franciscan Complex, a Jurassic–Cretaceous accretionary prism complex, renowned for earthflows and deep-seated landsliding (Iverson and Major, 1987; Kelsey, 1978). Some of the most extensive earthflow activity in northern California occurs along the main stem of the Eel River and its tributaries between Dos Rios and Alderpoint (Brown and Ritter, 1971). Highly erodible Central Belt mélange and high seasonal rainfall predispose this section of the Eel River to ubiquitous earthflows. Here we observe slow-moving landslides spanning all states of activity and form, from small <100 m² slumps, to huge earthflow complexes spanning 900 m of relief and extending as much as 5 km from channel to ridge.

We focused on a 1.5-km-long active earthflow (0.2 km² area) entering Kekawaka Creek, an 85 km² tributary of the Eel River (Fig. 1). This active earthflow has classic morphology (Keefer and Johnson, 1983), including a steep, amphitheater-like source area; a narrow, elongate transport zone that overrides several bedrock steps; and termination at the creek as a bulbous toe (Fig. DR1 in the GSA Data Repository¹). Specifically, we study the upper half of the earthflow where the surface has minimal disturbance and little lateral input from creeks and other earthflows. Based on morphology, we subdivide it into three kinematic units: a steep headscarp or source area, a long narrow transport zone, and a mid-slide compressional zone with reduced topographic gradient (Fig. 1). The headscarp of the earthflow currently abuts a broad ridgeline, underlain by sandstone.

HISTORICAL AIR PHOTOS AND SURVEYING

We use several approaches to study movement of the Kekawaka earthflow. Underpinning the analysis is high-resolution (1 m grid spacing) digital topography derived from airborne laser scanning (LiDAR, light detection and ranging) that reveals earthflow morphology

¹GSA Data Repository item 2009197, aerial photograph and orthorectification information (Table DR1), meteoric ¹⁰Be data (Table DR2), earthflow geomorphology (Fig. DR1), and error analysis of photograph orthorectification (Fig. DR2), is available online at www.geosociety.org/pubs/ft2009.htm, or on request from editing@geosociety.org or Documents Secretary, GSA, P.O. Box 9140, Boulder, CO 80301, USA.

*E-mail: bmackey@uoregon.edu.

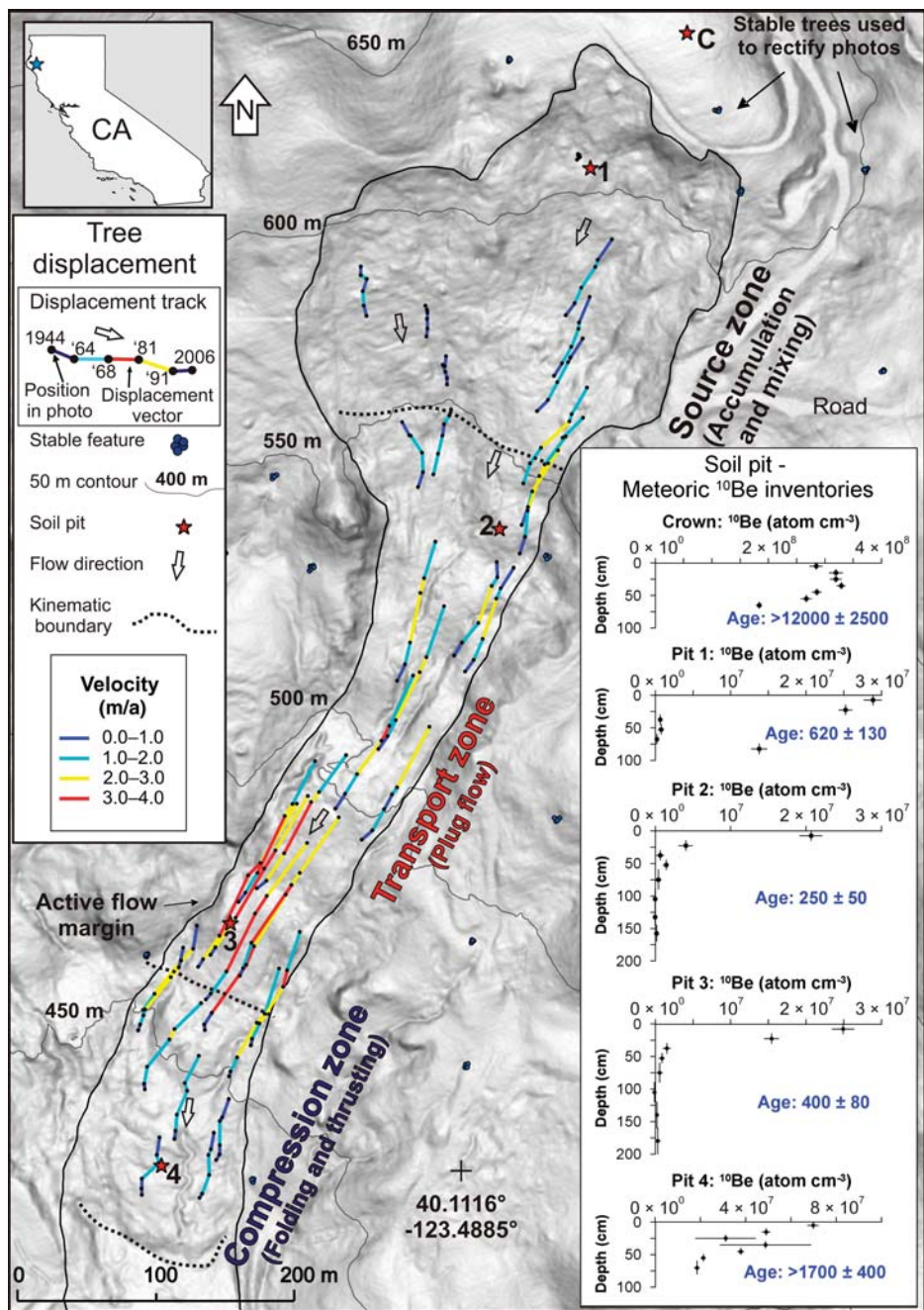


Figure 1. Colored lines show trajectories of trees growing on earthflow from 1944 to 2006, which we demarcate into three kinematic units. Inset shows depth profiles of meteoric ^{10}Be concentration. Vertical error bars show sample interval, and horizontal bars analytical error. Background image is light detection and ranging (LiDAR)-derived slope (1 m resolution). Inset map shows site location in northern California.

in unprecedented detail (Fig. 1; Fig. DR1). To determine modern earthflow movement, we placed 27 0.9 m rebar stakes on the slide, and recorded their positions using a total station for three successive summers (2006–2008).

To quantify decadal-scale slide deformation, we rectified historical air photos to remove lens distortions and topographic effects (Wolf and Dewitt, 2000) and measured offset features in sequential photographs (Baum et al., 1998,

Walstra et al., 2007). We obtained aerial photos taken in 1944, 1964, 1968, 1981, in addition to the LiDAR coverage flown in 2006, defining five time intervals of landslide change (Table DR1). We identified 53 individual trees growing on the earthflow surface and tracked their positions (and thus velocities) from 1944 to 2006 (Figs. 1 and 2). The sequential location of trees on stable ground adjacent to the earthflow enabled us to define errors due to

imperfect rectification or vegetation change (Fig. DR2).

METEORIC ^{10}Be AND THE TRANSPORT ZONE “SOIL CONVEYOR”

Based on field and LiDAR observations, we envisage the earthflow transport zone as a relatively undeformed “soil conveyor” that progressively translates material generated and mixed in the source area to the compressional zone. Because it can take hundreds to thousands of years for soil to move through an earthflow, we use a novel application of meteoric ^{10}Be that has the potential to substantially extend historical records of earthflow movement.

Meteoric ^{10}Be is produced in the atmosphere by the spallation (fragmentation) of atmospheric gas nuclei from cosmic rays (Monaghan and Elmore, 1994). Once produced, ^{10}Be (half-life of 1.51×10^6 years) attaches to submicron aerosol particles in the atmosphere. These particles are scavenged by precipitation, and delivered to the Earth’s surface. The ^{10}Be nuclide is rapidly adsorbed and sequestered when it contacts fine-grained soils, which typically have a high surface area per volume, and high cation exchange capacity (McKean et al., 1993; Pavich et al., 1986; You et al., 1989). ^{10}Be can be lost through groundwater leaching or clay translocation to lower soil horizons (Pavich et al., 1986), and is readily mobilized under acidic soil conditions. Soils derived from the Central Belt Franciscan mélange are ideal reservoirs for ^{10}Be because they are clay rich and relatively nonacidic.

By measuring the inventory of ^{10}Be through soil profiles and dividing by the annual ^{10}Be delivery rate, we calculated the age of several earthflow surfaces. Below the base of the steep source zone, which undergoes pervasive block rotation, ravel, and soil slips, the reconstituted earthflow material exhibits a broad, planar morphology, demarcating the top of the transport zone “soil conveyor.” At this location, we expect concentrations of ^{10}Be to be low, given the extent of source-zone reworking and thus dilution of previously stable ^{10}Be -enriched soil incorporated into the earthflow. Through the transport zone, we assume that the surface remains relatively intact such that local inventories of ^{10}Be progressively increase downslope. The ratio of the distance between two sample locations and the difference in their surface ages provides an estimate of the long-term velocity of the transport zone.

For this approach, we assume the following: (1) rainfall and ^{10}Be production are relatively constant with time, (2) minimal ^{10}Be is lost once it adheres to the soil (e.g., via leaching), (3) the cation adsorption capacity of the soil is not exhausted, and (4) slide movement occurs by simple plane strain. Below the headscarp, incomplete mixing of previously stable surface

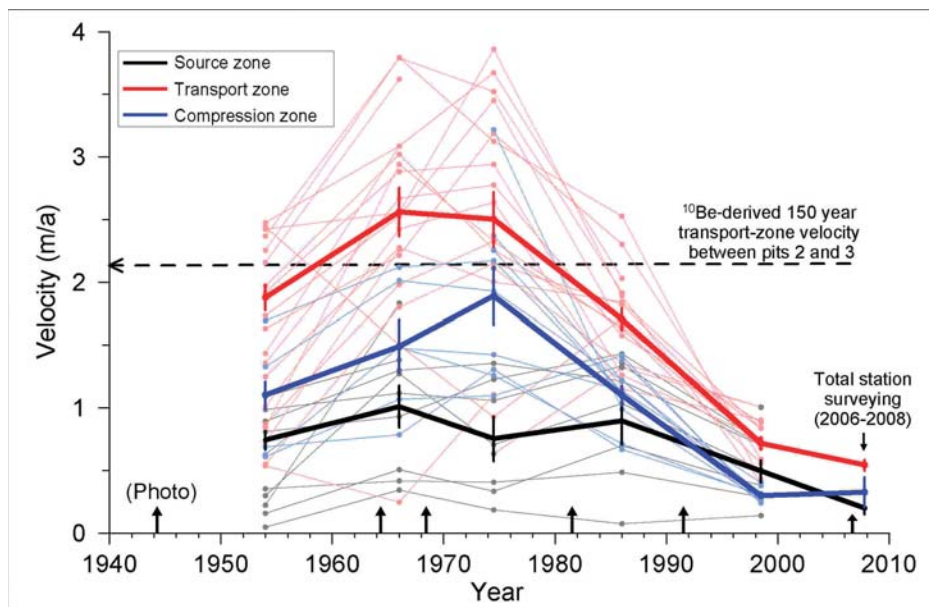


Figure 2. Tree velocities for three kinematic zones of earthflow for each photo interval, in addition to 2006–2008 total station survey data. We plot individual velocity of each tree (faint lines), and mean and standard error for each kinematic unit (bold lines).

soils with high ^{10}Be concentrations may cause pockets of concentrated ^{10}Be to persist. Such pockets should be readily identifiable because the progressive accumulation of ^{10}Be in stable, clay-rich surfaces tends to generate well-behaved exponential concentration profiles.

We dug four soil pits along the axis of the earthflow, and one on unfailed terrain above the headscarp crown (pit C, Fig. 1). The earthflow material is colluvium (poorly sorted gravelly clayey sand with occasional large rocks 1–5 m in diameter), whereas the soil above the headscarp was a loamy sand. We sampled soil at regular depth intervals in each pit, and collected intact samples to determine representative bulk density of the earthflow colluvium ($2.1 \pm 0.1 \text{ g/cm}^3$). We extracted ^{10}Be from the soil samples at the University of Washington Cosmogenic Isotope Laboratory, following the soil fusion technique described in Stone (1998). The $^{10}\text{Be}/^9\text{Be}$ ratio was analyzed via mass spectrometry at PRIME Lab, Purdue University. By integrating through the concentration profile, we calculated the inventory of ^{10}Be for each sample site (atoms/cm²). We used the average annual rainfall recorded at Alderpoint (15 km northwest) of $1.3 \text{ m} \pm 0.06$ (mean \pm standard error, 1940–1980) and an estimate for mid-latitude meteoric ^{10}Be production of $1.3 \times 10^6 \pm 20\%$ atoms/cm²/a per meter of rain (Pavich et al., 1986; Pavich and Chadwick, 1997) to quantify the surface exposure age of the earthflow soil.

RESULTS

Our surveying and photographic data show that earthflow velocities vary significantly

between the three kinematic units (Figs. 1 and 2). Maximum slide velocities averaged across each kinematic zone are lowest in the upper source zone ($<1 \text{ m/a}$), fastest through the narrow transport zone (2.5 m/a), and moderate through the mid-slide compressional zone (1.8 m/a). Since 1944, the average velocity in the transport zone has been 1.7 m/a, although temporal variation was substantial. Velocities were highest in the late 1960s and 1970s and have steadily decreased to $<1 \text{ m/a}$ since. This temporal pattern is broadly consistent over all three kinematic units (Fig. 2). The headscarp exhibited negligible expansion over the photographic record, whereas the mid-slope toe advanced more than 40 m.

Our ^{10}Be analysis (Fig. 1; Table DR2) demonstrates that the unfailed soil above the headscarp (pit C) has the highest inventory of ^{10}Be and a minimum surface age of 12 ka. On the earthflow, pits 1–3 show that the majority of ^{10}Be is retained in the upper 40 cm of soil, although pit 1 in the source zone has an anomalous high concentration at 90 cm. Pits 2 and 3 in the transport zone show a difference in surface age of $150 \pm 90 \text{ a}$, which can be used to derive a long-term slide velocity of $2.1 \pm 1.3 \text{ m/a}$ (Figs. 1 and 2). Pit 4, in the compression zone, retained $1700 \pm 400 \text{ a}$ of ^{10}Be , although this age remains a minimum estimate, as our deepest sample interval shows high concentrations of ^{10}Be , implying that the isotope has penetrated to depths below 90 cm.

DISCUSSION AND CONCLUSIONS

The spatial pattern of movement, as revealed by photo-derived tree displacement vectors

(Fig. 1), shows a systematic change in displacement rates from the headscarp to the lower portion of the earthflow. The upper source zone exhibits slowing velocities of $\sim 1 \text{ m/a}$, indicative of slow steady input of source material from headscarp slumping. The maximum earthflow velocities are obtained through the narrow (80 m wide) section of the transport zone. This section also has the smoothest surface, largely free of folding or extensional slumping, implying plug sliding with minimal internal deformation (Fig. DR1). The mid-slope compressional zone exhibits slower movement than the transport zone, but follows a similar temporal pattern. Here the slide widens and has a series of folds and thrusts that reflects deformation from the advancing transport zone.

Although we do not have well-delimited data on the basal sliding depth, field-based estimates from the channel margin of the Kekawaka slide are $\sim 6 \text{ m}$, and similar sized earthflows have depths in the range of 4–8 m (Iverson and Major, 1987; Zhang et al., 1991). Taking an average velocity of 2 m/a, the earthflow translates over $1000 \text{ m}^3/\text{a}$ through the transport zone. Given that the combined area of the earthflow source and transport zones is $1.0 \times 10^5 \text{ m}^2$, sliding at 2 m/a equates to an average lowering rate of 10 mm/a, more than 20 times faster than the estimated regional erosion rate (Fuller et al., 2009). The evacuated volume of the earthflow source area and transport zone is $\sim 1.0 \times 10^6 \text{ m}^3$, suggesting that $\sim 1000 \text{ a}$ are required to evacuate the earthflow basin given average transport zone sliding of 2 m/a.

The inventories of ^{10}Be provide crucial insight about the long-term evolution of the landslide. Pit C on the unfailed surface above the headscarp has the highest ^{10}Be inventory, as would be expected for stable ground. Given the sandy nature of the soil at this location, some of the ^{10}Be may have been lost from this pit, probably by leaching. Pit 1 is within the steep, unstable part of the accumulation zone amid back-rotated headscarp slumps and disintegrating blocks of detached argillaceous bedrock. As such, we interpret much of the pit 1 inventory and concentration spike at 80–90 cm to be residual headscarp soil that has yet to be fully mixed or buried, indicating that pit 1 reflects a transient state between headscarp failure and reconstituted earthflow surface.

Owing to their location in the transport zone, pits 2 and 3 are useful for determining long-term rates of earthflow movement. Both show that the majority of ^{10}Be is retained within the upper 40 cm, and these pits have negligible ^{10}Be below this depth. We argue that ^{10}Be at these sites began accumulating when the surface moved into the transport zone, which is dominated by translational movement as opposed to the mixing in the source zone. Our ^{10}Be -derived

prehistoric velocity (2.1 m/a) exceeds the 62 a average transport zone velocity obtained from the photos (1.7 m/a), and, to account for the reduced velocities over the past 30 years, the transport zone may have sustained velocities approaching 2.5 m/a prior to 1944.

Pit 4 has 1700 ± 400 a of ^{10}Be . The pit 4 ^{10}Be depth profile shows ^{10}Be concentration decreasing in a noisy exponential fashion, and the isotope has penetrated to depths well below 40 cm, and probably below our deepest sample at 90 cm. The pit 4 age represents a minimum age of the earthflow. The transport rate between pits 3 and 4 is ~ 0.15 m/a, and the earthflow has longitudinally shortened through this section via compression and widening, which may account for much of the deceleration. Air photo-derived velocities in this area exceed 1 m/a, suggesting that earthflow movement is episodic and the earthflow surface proximate to pit 4 may have originally been formed during a previous episode of activity, and has subsequently been reactivated, all the while continuing to accumulate ^{10}Be .

The acceleration and subsequent gradual slowing of the 1944–2006 vectors illustrates the nonsteady nature of this earthflow's movement at the decadal scale, probably due to climatic variation, supporting the notion of episodic or surging behavior superimposed on the long-term earthflow evolution. Historical increases in earthflow activity have colloquially been attributed to anthropogenic activity such as grazing, but the dramatic slowing of the Kekawaka earthflow does not support this contention. The peak velocities recorded from 1964 through 1981 coincide with both increases in rainfall and discharge across the Eel River catchment in the mid-twentieth century (Syvitski and Morehead, 1999) and a large storm event in 1964.

Regardless of climatic forcing, a supply of readily mobilized source material is requisite for continued earthflow movement. The Kekawaka earthflow headscarp has retrogressed to a sandstone ridgeline, likely limiting or greatly slowing future expansion, and the source zone has received minimal fresh material since the 1940s. With continued earthflow movement (and assuming no downward propagation of the failure surface), the slide thickness must have decreased, causing a reduction in shear stress. This supply limitation may be a primary factor in the long-term velocity decline revealed by our analysis, although the buttress-

ing effect of accumulation in the low-gradient mid-slope compressional zone may also contribute. The surface of the earthflow is 5–10 m lower than the surrounding slopes, consistent with progressive deflation and slowing of the active slide. Given this supply limitation, the Kekawaka earthflow appears set to become a dormant feature, typical of this slide-dominated landscape.

ACKNOWLEDGMENTS

This research was funded by National Science Foundation grant EAR-0447190 to Roering, Mackey was partially supported by the Fulbright EQC Award in Natural Disaster Research from New Zealand. The LiDAR data were acquired by the National Center for Airborne Laser Mapping (NCALM). John Stone, Greg Balco, and the University of Washington Cosmogenic Isotope Laboratory provided invaluable advice and assistance with ^{10}Be processing. We thank Calvin and Wendy Stewart for field access and generous hospitality. Sean Bemis, Adam Booth, and Laura Stimely provided assistance with field surveying. Discussions with Harvey Kelsey enhanced our understanding of this spectacular landscape.

REFERENCES CITED

Baum, R.L., Messerich, J., and Fleming, R.W., 1998, Surface deformation as a guide to kinematics and three-dimensional shape of slow-moving, clay-rich landslides, Honolulu, Hawaii: *Environmental and Engineering Geoscience*, v. 4, p. 283–306.

Bovis, M.J., and Jones, P., 1992, Holocene history of earthflow mass movements in south-central British Columbia—The influence of hydroclimatic changes: *Canadian Journal of Earth Sciences*, v. 29, p. 1746–1755.

Brown, W.M., and Ritter, J.R., 1971, Sediment transport and turbidity in the Eel River Basin, California: U.S. Geological Survey Water-Supply Paper 1986, 70 p.

Coe, J.A., Ellis, W.L., Godt, J.W., Savage, W.Z., Savage, J.E., Michael, J.A., Kibler, J.D., Powers, P.S., Lidke, D.J., and Debray, S., 2003, Seasonal movement of the Slumgullion landslide determined from Global Positioning System surveys and field instrumentation, July 1998–March 2002: *Engineering Geology*, v. 68, p. 67–101, doi: 10.1016/S0013-7952(02)00199-0.

Dietrich, W.E., and Perron, J.T., 2006, The search for a topographic signature of life: *Nature*, v. 439, p. 411–418, doi: 10.1038/nature04452.

Fuller, T.K., Perg, L.A., Willenbring, J.K., and Lepper, K., 2009, Field evidence for climate-driven changes in sediment supply leading to strath terrace formation: *Geology*, v. 37, p. 467–470, doi: 10.1130/G25487A.1.

Iverson, R.M., and Major, J.J., 1987, Rainfall, ground-water-flow, and seasonal movement at Minor Creek landslide, northwestern California—Physical interpretation of empirical relations: *Geological Society of America Bulletin*, v. 99, p. 579–

594, doi: 10.1130/0016-7606(1987)99<579:RGFASM>2.0.CO;2.

Keefer, D.K., and Johnson, A.M., 1983, Earth flows: Morphology, mobilization and movement: U.S. Geological Survey Professional Paper 1256, 56 p.

Kelsey, H.M., 1978, Earthflows in Franciscan melange, Van Duzen River basin, California: *Geology*, v. 6, p. 361–364, doi: 10.1130/0091-7613(1978)6<361:E1FMVD>2.0.CO;2.

McKean, J.A., Dietrich, W.E., Finkel, R.C., Southon, J.R., and Caffee, M.W., 1993, Quantification of soil production and downslope creep rates from cosmogenic ^{10}Be accumulations on a hill-slope profile: *Geology*, v. 21, p. 343–346, doi: 10.1130/0091-7613(1993)021<0343:QOSPAD>2.3.CO;2.

Monaghan, M.C., and Elmore, D., 1994, “Garden variety” ^{10}Be in soils on hill slopes: Nuclear Instruments and Methods in Physics Research Section B, Beam Interactions with Materials and Atoms, v. 92, p. 357–361, doi: 10.1016/0168-583X(94)96034-8.

Pavich, M.J., and Chadwick, O.A., 1997, ^{10}Be soil inventories along a climatic gradient on Kohala Mountain: *Geological Society of America Abstracts with Programs*, v. 29, no. 5, p. 56.

Pavich, M.J., Brown, L., Harden, J., Klein, J., and Middleton, R., 1986, ^{10}Be distribution in soils from Merced River terraces, California: *Geochimica et Cosmochimica Acta*, v. 50, p. 1727–1735, doi: 10.1016/0016-7037(86)90134-1.

Stone, J., 1998, A rapid fusion method for separation of beryllium-10 from soils and silicates: *Geochimica et Cosmochimica Acta*, v. 62, p. 555–561, doi: 10.1016/S0016-7037(97)00369-4.

Syvitski, J.P., and Morehead, M.D., 1999, Estimating river-sediment discharge to the ocean: Application to the Eel margin, northern California: *Marine Geology*, v. 154, p. 13–28, doi: 10.1016/S0025-3227(98)00100-5.

Walstra, J., Dixon, N., and Chandler, J.H., 2007, Historical aerial photographs for landslide assessment: Two case histories: *Quarterly Journal of Engineering Geology and Hydrogeology*, v. 40, p. 315–332, doi: 10.1144/1470-9236/07-011.

Wolf, P.R., and Dewitt, B.A., 2000, Elements of photogrammetry: With applications in GIS (third edition): Boston, Massachusetts, McGraw-Hill, 608 p.

You, C.F., Lee, T., and Li, Y.H., 1989, The partition of Be between soil and water: *Chemical Geology*, v. 77, p. 105–118, doi: 10.1016/0009-2541(89)90136-8.

Zhang, X.B., Phillips, C., and Pearce, A., 1991, Surface movement in an earthflow complex, Raukumara Peninsula, New Zealand: *Geomorphology*, v. 4, p. 261–272, doi: 10.1016/0169-555X(91)90009-Y.

Manuscript received 13 February 2009
 Revised manuscript received 25 April 2009
 Manuscript accepted 28 April 2009

Printed in USA